On the influence of the numerical strategy on the predictive character of Euler-Euler models for two-phase flow simulations in solid rocket motor instabilities

Valentin Dupif, Marc Massot, Joel Dupays, Frédérique Laurent, Clément Le Touze

On the influence of the numerical strategy on the predictive character of Euler-Euler model for two-phase flow simulations in solid rocket motor instabilities

Valentin Dupif[1,2,3] [*], Marc Massot[1,2,3], Joël Dupays[1], Frédérique Laurent[2,3] and Clément Le Touze[1]

[1] *Département Energétique Fondamentale et Appliquée - DEFA*
ONERA Chemin de la Hunière 91123 Palaiseau FRANCE
valentin.dupif@onera.fr , joel.dupays@onera.fr , clement.le_touze@onera.fr

[2] *Laboratoire EM2C UPR 288, CNRS, CentraleSupélec, Université Paris-Saclay*
Grande Voie des Vignes 92295 Châtenay-Malabry FRANCE
marc.massot@centralesupelec.fr , frederique.laurent@centralesupelec.fr

[3] *Fédération de Mathématiques de l'Ecole Centrale Paris, FR CNRS 3487*
Grande Voie des Vignes 92295 Châtenay-Malabry FRANCE

Abstract

Solid Rocket Motors involve strongly coupled two-phase flow. The presence of a polydisperse spray of particles resulting from the combustion of aluminized propellant has been shown to have a strong impact on stability and can eventually yield thrust oscillations. The ability to conduct predictive simulations of such a harsh environment is highly desirable. Euler-Euler models relying on moment methods for the disperse phase constitute interesting approaches due to their efficiency at coupling both phases and their ability for high performance computing. A multi-fluid model coupled to a new numerical strategy for the disperse phase is introduced in order to cope with the natural high stiffness of the resulting systems of conservation laws. The predictive character of the method is strongly related to the possibility of using accurate methods while preserving stability and robustness in the presence of intrinsic singularities occurring in the disperse phase equations. The purpose of this contribution is to stress the impact of several numerics and modeling on the solution. Relevant test cases for solid propulsion involving hydrodynamic instabilities and acoustic coupling are presented. A strategy is proposed in order to produce reliable predictions.

Keywords: Solid rocket motor, Vortex shedding, Two-way coupling, Euler-Euler simulation, Velocity polydispersion, Anisotropic Gaussian, Realizable high order schemes

1. Introduction

Among the space propulsion technologies, Solid Rocket Motors (SRM) are known for their reliability, high trust and ability to be stored during a long period of time. Included their relatively low cost, such engines are first choice possibilities for the first stages of present and future space launchers[8]. In order to improve their efficiency, or more particularly their specific impulse, aluminum powder is added to the propellant grain increasing the temperature of the burnt mixture. From this technical solution results the presence of a massive amount of aluminum oxide particles that strongly interact with the internal flow of the motor. Since these particles have a notable impact on thermo-acoustic, combustion and hydrodynamic instabilities or combination of these [12], it is a key issue to be able to prevent such phenomenon in the early development of solid rocket motor and thus avoid deleterious effects on the launcher mission.

Due to the harsh conditions existing in the internal flow, measurement possibilities are limited and simulations are mandatory. In addition to the experimental investigations to understand the complex physic of such flows, the ONERA continually refine the modeling of both carrier and disperse phase while improving associated numerical methods of CFD issues. This contribution exhibit the recent progress in the disperse phase modeling including its two-way interaction with the gaseous carrier phase obtained thanks to a long term collaboration with the EM2C laboratory of CentraleSupelec [4, 21]. This work is focused on the Eulerian representation of polydisperse [4, 14] spray giving solution for realistic flow of particles taking into account a large spectrum of size of droplets [6] and more recently statistical droplet trajectory crossing [25, 20]. The ultimate goal of these works is to produce models that can efficiently represent particles from low to high inertia. While being mathematically well posed, such models are exposed to severe non-linearities and have to rely on dedicated numerical methods. In order to aim at industrial configurations, an active research is conducted on accurate and robust numerical methods for unstructured mesh [15] constantly improving the reliability of computed solutions. In our recent work, a discriminant test case under a realistic configuration for SRMs is investigated and will be the key point of this paper. Highly sensitive to the numerical method, this fictive SRM, namely C1 [17, 18, 11], possesses an intrinsic purely hydrodynamic instability that can be either excited, reduced or even suppressed by the single presence of particles under a condensed form. Through this new analysis of the problem, we propose to distinguish the spurious phenomena associated to the numerical method from those attributable to the model.

The contribution is organized as follow. Section 2 is devoted to the modeling of the disperse phase according to the briefly described SRM's internal flow conditions. From the closure of the kinetic description of the particles, two Eulerian models are deduced and will form our governing equations solved thanks to the numerical methods proposed in section 3. Special care is taken of the design of robust schemes conserving the mathematical properties of the models while keeping a high precision. Then Section 4 introduces the two-phase C1 test case that will assess the relia-

[*] The present research was conducted thanks to a Ph.D. Grant from ONERA. This work relies on a long-term collaboration work between EM2C laboratory and the Fundamental and Applied Energetics (DEFA) department at ONERA. Support from ONERA is gratefully acknowledged.

bility of models and methods. The ability of our configuration to be predictive will be the subject final discussions leading to the conclusion of the paper.

2. Model

The internal flow of a SRM involves complex phenomena that can interact with each other. This includes for instance combustion, turbulence and radiative heat transfer, but in this paper, acoustics and two-phase flow issues will be our only concern. This choice of simplicity is motivated by the two-phase C1 test case that will be introduced in another Section 4. We then focus on the description of the disperse phase and its interaction with the carrier phase. After arguing on the choice of an Euler-Euler model, two kinetic closures are proposed for the disperse phase and the governing equations obtained thanks to a method of moment.

2.1. Eulerian model of the flow

Combustion and multi-component gas issues are omitted to simplify the study. The compressible form of the well known Navier-Stokes equations is retained. Since it has been proven that LES models have a marginal impact in the case of a C1 configuration without particles [11], the equations will be solved under a DNS context.

Combined with their high material density, the small size of the droplets justify the assumption of point-particle. Through a diameter lying between several hundred of nanometers and few hundred of micrometers, their volume fraction in the Navier-Stokes equations can be neglected. Thus only two kinds of interactions between the carrier and carried phase are considered, namely the drag force and the heat exchange. According to [2], the Reynolds number of the droplets remain under 500 even through the nozzle, where it is the highest, and classical Schiller-Naumann and Ranz-Marshall corrections are sufficient to describe the dynamics of an isolated particle. These take the following form:

$$\begin{cases} \boldsymbol{F^{St}}(\boldsymbol{u}_g, \boldsymbol{c}, d_p) = \frac{(\boldsymbol{u}_g - \boldsymbol{c})}{\tau_u^{st}}, \quad \tau_u^{st} = \frac{\rho_l d_p^2}{18\mu_g} \\ \boldsymbol{F} = \boldsymbol{F^{St}}(1 + 0.15Re_p^{0.687}) = \frac{(\boldsymbol{u}_g - \boldsymbol{u}_p)}{\tau_u} \end{cases} \tag{1}$$

$$\begin{cases} H^{St}(T_p, T_g, d_p) = c_{p,l}\frac{T_g - T_p}{\tau_T^{st}}, \quad \tau_T^{st} = \frac{3}{2}Pr_g\frac{c_{p,l}}{c_{p,g}}\tau_u^{st} \\ H = H^{St}(1 + 0.3Re_p^{1/2}Pr_g^{1/3}) = c_{p,l}\frac{T_g - T_p}{\tau_T} \end{cases} \tag{2}$$

where $\boldsymbol{F}$ and H are given by unit of mass, $\boldsymbol{u}_g$ and $\boldsymbol{c}$ are the velocities of the gas and the particle, ρ_l is the density of the droplet material, d_p the diameter of the droplet, μ_g the dynamical viscosity of the gas, Re_p the Reynolds number of the particle, Pr_g the Prandtl of the gas and finally $c_{p,g}$ and $c_{p,l}$ the heat capacity at constant pressure of the gas and the droplet material.

The number of particles, that can easily reach 10^5 per cubic centimeter, induces a non negligible collisions frequency [3]. Such a problem is out of the scope of the paper and will be neglected. The droplets are then consider only to be able to interact between themselves through their coupling with the gaseous phase.

At this point, two classes of models for the resolution of the disperse phase can be considered. It can be described through a Lagrangian method where droplets are tracked, alone or grouped, in their displacement or thanks to a Eulerian framework by describing droplets through local quantities. For phenomena driven by two-way interactions as in the SRMs, one may prefer the Eulerian framework. As a matter of fact such method can accurately calculate droplet-gas interaction with a precision that does not depend on their number while avoiding statistical convergence issues. This last property is a key advantage for two-way coupled unsteady simulations. Moreover, Eulerian closure can be efficiently parallelized through domain decomposition whereas Lagrangian methods quickly suffer from memory exchange overhead in the same situation.

Then, assuming the statistical convergence through an infinite number of particles, the spray can be described thanks to a Number Density Function (NDF) f that depends on the time t, position $\boldsymbol{x}$, velocity $\boldsymbol{c}$ and temperature T. This simplified form of the Williams-Boltzmann equation assumes a unique particle size without evaporation nor collision terms and take the following form:

$$\underbrace{\partial_t f + \partial_x.(cf)}_{\text{free transport}} + \underbrace{\partial_c.(\boldsymbol{F}_n f)}_{\text{drag force}} + \underbrace{\partial_T(\frac{H_n}{c_{p,l}} f)}_{\text{thermal transfert}} = 0 \tag{3}$$

where $\boldsymbol{F}_n$ and H_n are the drag force and heat transfer applied to a single droplet. This model is not solved directly but approximated through moment methods.

2.2. Kinetic based moment method

Equations are written on moments in velocity and temperature. Despite our choice of considering only a discrete size of particles, we wish to be able to extend the presented work to two size-moment hybrid methods [1, 3, 14]. These methods use a size discretization into sections [12] and two size-moments in each section and have reach a mature level but are out of the scope of this paper (see [6, 14, 1] and references therein for a broader view on the literature in this field). Then, the number density $n = \int f \mathrm{d}\boldsymbol{c}\mathrm{d}T\mathrm{d}S$ and the mass density m are considered, despite their redundancy, as proof of feasibility and straightforward extension of the presented work to such literature. Therefore, the particle diameter d_p will not be considered as a fixed parameter but as deduced from n and m thanks to the formula $d_p = [(6m)/(\rho_l \pi n)]^{1/3}$.

We propose then to close problem thanks to assumptions on the NDF according to the velocity and temperature at a time t and position $\boldsymbol{x}$. Assuming that these two local variables can be closed independently, the NDF can be stated as follow:

$$f(t, \boldsymbol{x}, \boldsymbol{c}, T) = n(t, \boldsymbol{x}) f_{\boldsymbol{c}}(t, \boldsymbol{x}, \boldsymbol{c}) f_T(t, \boldsymbol{x}, T) \tag{4}$$

Assuming this explicit form of f, conservation laws can be obtained thanks to the transport equation (3): from the integration of (3), one can obtain sets of equations with usual physical meanings. Thus, the moments of order 1 and 2 in velocity lead to the conservation of momentum and kinetic energy, the moment of order 1 in temperature leads to the conservation of the thermal energy and the zeroth order moment to the conservation of particle number and mass.

For the sake of simplicity, a discrete temperature of the particle T_p at a point is assumed, which leads to $f_T(t, \boldsymbol{x}, T) = \delta\left(T - T_p(t, \boldsymbol{x})\right)$. After the integration of (3) multiplied by the temperature T and the heat capacity $c_{p,l}$, one can obtain the equation of the transport of the thermal energy $h = c_{p,l}T_p$ such as:

$$\partial_t\left(mh\right) + \partial_{\boldsymbol{x}} \cdot \left(mh\boldsymbol{u}\right) = mc_{p,l}\frac{T_g - T_p}{\tau_T} \tag{5}$$

where $\boldsymbol{u}$ is the average velocity obtained for the first moment in velocity $\boldsymbol{u} = n^{-1}\int \boldsymbol{c} f \mathrm{d}\boldsymbol{c}\mathrm{d}T\mathrm{d}S$.

The form of the velocity distribution will be a key point of this contribution. It is possible to consider locally a unique velocity such as $f_{\boldsymbol{c}}(t, \boldsymbol{x}, \boldsymbol{c}) = \delta\left(\boldsymbol{c} - \boldsymbol{u}(t, \boldsymbol{x})\right)$, which will be called the monokinetic (MK) assumption [13]. This hypothesis results in the equations of Pressureless Gas Dynamic (PGD) with a drag source terms on the right hand side. Combined with the conservation of energy (5) and particle number, one can obtain the system that follow:

$$\begin{cases} \partial_t n + \partial_{\boldsymbol{x}} \cdot (n\boldsymbol{u}) & = 0 \\ \partial_t m + \partial_{\boldsymbol{x}} \cdot (m\boldsymbol{u}) & = 0 \\ \partial_t (m\boldsymbol{u}) + \partial_{\boldsymbol{x}} \cdot (m\boldsymbol{u} \otimes \boldsymbol{u}) & = m\frac{\boldsymbol{u}_g - \boldsymbol{u}}{\tau_u} \\ \partial_t (mh) + \partial_{\boldsymbol{x}} \cdot (mh\boldsymbol{u}) & = mc_{p,l}\frac{T_g - T_p}{\tau_T} \end{cases} \tag{6}$$

The monokinetic assumption finds its limits for relatively inertial droplets for which Particle Trajectory Crossing (PTC) [2] can occur. In other word, the particles belonging to the same system of equations cannot cross each other at a given point. This uniqueness of the local velocity created in case of PTC a Dirac delta function in density called δ-shock. To avoid such drawback, recent works inspired by the theory of rarefied gas [16] proposed a multivariate Gaussian distribution in velocity [25, 19, 20] $f_{\boldsymbol{c}}(t, \boldsymbol{x}, \boldsymbol{c}) = \frac{det(\boldsymbol{\Sigma})^{-1/2}}{(2\pi)^{\frac{1}{2}N_d}} exp(-\frac{1}{2}(\boldsymbol{u}-\boldsymbol{c})^T\boldsymbol{\Sigma}^{-1}(\boldsymbol{u}-\boldsymbol{c}))$ where $\boldsymbol{\Sigma}$ is the covariance matrix of the velocity. Using the moment in velocity up to the order 2, one can obtain:

$$\begin{cases} \partial_t n + \partial_{\boldsymbol{x}} \cdot (n\boldsymbol{u}) & = 0 \\ \partial_t m + \partial_{\boldsymbol{x}} \cdot (m\boldsymbol{u}) & = 0 \\ \partial_t (m\boldsymbol{u}) + \partial_{\boldsymbol{x}} \cdot (m\boldsymbol{u} \otimes \boldsymbol{u} + \mathbb{P}) & = m\frac{\boldsymbol{u}_g - \boldsymbol{u}}{\tau_u} \\ \partial_t (m\mathbb{E}) + \partial_{\boldsymbol{x}} \cdot ((m\mathbb{E} + \mathbb{P}) \vee \boldsymbol{u}) & = m\frac{\boldsymbol{u}_g \vee \boldsymbol{u} - 2\mathbb{E}}{\tau_u} \\ \partial_t (mh) + \partial_{\boldsymbol{x}} \cdot (mh\boldsymbol{u}) & = mc_{p,l}\frac{T_g - T_p}{\tau_T} \end{cases} \tag{7}$$

where $\mathbb{E}$ is the energy matrix and $\mathbb{P}$ the granular pressure tensor defined by $\mathbb{P} = m\boldsymbol{\Sigma} = 2m\mathbb{E} - m\boldsymbol{u} \otimes \boldsymbol{u}$.

This second system, called AG for Anisotropic Gaussian, is an extension of the MK system. As a matter of fact, the system (6) based on the MK closure is contained in (7) in the limit of zero velocity dispersion. A first analysis of the left hand side of the system (7) shows that the nature of this system of this Partial Differential Equations (PDE) is hyperbolic as the compressible Navier-Stokes chosen for the gas. These equations require specific methods of resolution since they contain intrinsic singularities such as shock waves. In the case of the system (6), the left hand side is a weakly hyperbolic PDE, which means that the Jacobian of the matrix is not invertible. From this specificity, result the strong singularity that is the δ-shock. The remaining part of the equations that is the right hand side of the chosen system and its backward action on the carrier phase act as a simple system of ODEs. Since both models possess their own properties, they have to rely on adapted numerical methods in order to produce accurate solutions.

3. Numerical methods

For the sake of genericity, the involved equations (6) or (7) and the Navier-Stokes equations are split into three operators. The right hand side of the equations (6) (or (7)) as well as their action on the carrier phase will be treated as a source term operator $\mathcal{S}$ and can be written as an ODE $\mathrm{d}_t\boldsymbol{U} = S(\boldsymbol{U})$ where S is the source term function acting on the conservative vector $\boldsymbol{U}$. In the same way $\mathcal{T}_g$, $\mathcal{T}_p$ will be the transport operators corresponding to the usual Navier-Stokes equations and the left hand side of the equations (6) (or (7)) that can take the generic form $\partial_t\boldsymbol{U} + \partial_{\boldsymbol{x}} \cdot \boldsymbol{f}(\boldsymbol{U}) = 0$, where $\boldsymbol{f}$ is the flux function. After describing our splitting strategy as well as the treatment of the source terms, two methods for the resolution of the transport operators are proposed.

3.1. Operator splitting and source terms

Through a Strang splitting, the integration of the source terms is conducted independently from the resolution of the transport operators. Expecting steep source terms, we choose to use the operator $\mathcal{S}$ on half a time-step before solving independently the transport operators $\mathcal{T}_g$ and $\mathcal{T}_p$ since they are uncorrelated at this point and then conclude by half a time of source terms. Under a mathematical formulation, this gives:

$$\boldsymbol{U}^{Strang}(t+\Delta t) = \mathcal{S}\left(\frac{\Delta t}{2}\right)[\mathcal{T}_g + \mathcal{T}_p](\Delta t)\mathcal{S}\left(\frac{\Delta t}{2}\right)\boldsymbol{U}(t) \tag{8}$$

For the integration of the source terms, the use of a third order Strong Stability Preserving Runge-Kutta (SSPRK) time integration [7] is known to be a reliable choice. Combined with the Strang scheme, it leads to an efficient way to treat the source terms.

3.2. MacCormack method

Among the second order methods to solve hyperbolic systems of equations, the MacCormack method, of Lax-Wendroff class, has been very popular during the 80's and 90's thanks to its easiness of implementation and numerical efficiency. In an one dimensional framework, the scheme takes the compact predictor-corrector formulation that follow:

$$\begin{cases} \overline{\boldsymbol{U}}_i^n = \boldsymbol{u}_i^n + \frac{\Delta t}{\Delta x}(\boldsymbol{f}(\boldsymbol{U}_i^n) - \boldsymbol{f}(\boldsymbol{U}_{i-1}^n)) \\ \boldsymbol{U}_i^{n+1} = \frac{1}{2}\left[\boldsymbol{U}_i^n + \overline{\boldsymbol{U}}_i^n + \frac{\Delta t}{\Delta x}(\boldsymbol{f}(\overline{\boldsymbol{U}}_{i+1}^n) - \boldsymbol{f}(\overline{\boldsymbol{U}}_i^n)\right] \end{cases} \tag{9}$$

where $\overline{\boldsymbol{U}}_i^n$ is the solution at the predictor step that is here left oriented.

To our knowledge, every multidimensional application of the MacCormack method is linked to a structured mesh and a direction of the predictor according to the grid directions such as in [17]. The experience shows that this predictor should be oriented upstream which for SRMs means toward the propellant grain in the radial direction or toward the head-end in the axial direction. Such choice reduces the spurious oscillations but does not solve this issue. To ensure the quality of the results, an artificial viscosity of Swanson and Turkel [22] is chosen. The sensor is based on the pressure for the carrier phase but since this value is absent of the monokinetic closure and irrelevant for the AG, the density field is chosen instead. Such method fits well the requirement for the gaseous phase since purely acoustic phenomenon are expected to be observed and shocks avoided inside the internal flow. However the possibility of some vacuum area and discontinuity in the field of particles can lead to stability issues. Despite the solution should be smooth in most of the chamber, an high artificial viscosity is required to manage local singularities and vacuum. In consequence, the ability for this scheme to solve the disperse phase is ambiguous.

3.3. MUSCL method

Form the idea of solving discontinuities at the cell interfaces in a finite-volume context, the Godunov scheme class is proven to be able to efficiently tackle singularities. The procedure consists in estimating in a first time the value at the cell interface, then solving Riemann problems at the cell interfaces to deduce the flux while ensuring the entropy condition. In a one-dimensional framework the scheme takes the form:

$$\begin{cases} \boldsymbol{U}_i^{n+1} = \boldsymbol{U}_i^n + \frac{\Delta t}{\Delta x}\left(f(\boldsymbol{U}_{i+1/2}^{Ri}) - f(\boldsymbol{U}_{i-1/2}^{Ri})\right) \\ \boldsymbol{U}_{i+1/2}^{Ri} = \mathcal{U}^{Ri}(\frac{x}{t} = 0, \boldsymbol{U}_{i+1/2}^l, \boldsymbol{U}_{i+1/2}^r) \end{cases} \tag{10}$$

where $\boldsymbol{U}_{i+1/2}^{Ri}$ is the solution to the Riemann problem between the left state $\boldsymbol{U}_{i+1/2}^l$ and right state $\boldsymbol{U}_{i+1/2}^r$ solved by the procedure $\mathcal{U}^{Ri}$.

At order one, piecewise constant values are assumed in each cell equal to the average quantity contained in the corresponding volume and the extension to multidimensional frameworks is

straightforward. The resolution of the Riemann problem finds an explicit solution for the PGD equations [10]. However, such a procedure is tedious for more complex systems and we will rely on a HLLC approximate Riemann solver for the gas [24] and the HLL solver proposed in [25] for the AG equations. Each of them preserves the realizability as long as the reconstructed values are realizable states which is obvious at first order.

To obtain higher order schemes of this kind, the distribution of the value inside the cell have to be estimated. It can be achieved at the second order, for example, through a linear reconstruction leading to methods called MUSCL. For multidimensional frameworks, several procedures claim to be of MUSCL type. Among them the multislope method recently developed at ONERA [15] provides an efficient and robust Local Extrema Diminishing (LED) reconstruction [9]. When CFL independent, this LED property ensures that the reconstructed value will be a convex combination of its neighbors and will not create any artificial extrema. The key issue to obtain the realizability of such LED scheme, once the Riemann solver is proven realizable, is to select the right primitive value for the reconstruction that ensure the realizability of the deduced state.

LED reconstructions of the density and pressure fields ensure the positivity of these variables. Thus for the carrier phase, the density, the velocity and the pressure are usual choices ensuring the robustness. For the monokinetic closure, the choice of density and the velocity as reconstruction variables ensures the realizability [10]. Compared to the PGD equations, the AG closure needs, in addition, the positivity of the σ_{ij} component of the covariance matrix as well as the positivity of its determinant $\sigma_{ii}\sigma_{jj} - \sigma_{ij}^2 > 0 \quad \forall i \neq j$. As proposed in [25] the diagonal terms σ_{ii} are use for the reconstruction to ensure their positivity. However, we introduce here the new reconstruction value $\sigma_{ij}/\sqrt{\sigma_{ii}\sigma_{jj}}$ that have to be kept in $[0, 1[$ to ensure the previous constraints. The value of σ_{ij} deduced from this variable is then sure to fulfill the realizability requirement thanks to the LED procedure for its reconstruction and the positivity σ_{ii} and σ_{jj} as already provided. Finally, the knowledge acquired in the field of size polydispersion [10] suggests that the reconstruction over h and n/m prevent from any spurious border effect on the temperature and the size deduced from n and m.

Thanks to their design, these upwind methods are built-in realizable and robust with a L_∞ stability proven under CFL condition. This property is preserved through the second order SSPRK [7] time integration used to keep the convergence orders in space and time equal. In contrast to the MacCormack scheme where a case dependent manual tuning of the artificial viscosity is needed, these method lead to the exact solutions through mesh refinement without any artificial input. This property will be crucial for the analysis of the numerical solutions.

4. Two-phase C1 analysis

In industrial applications, propellant grain usually have sharp edges. The 2D planar C1 test case has been designed in order to reproduce a critical situation due to this geometrical singularity and asses the robustness of models and numerical methods. After having accurately described the case studied, the specific case where $20\mu m$ particles are injected is investigated.

4.1. Test case presentation

Downstream geometrical discontinuities on the propellant grain, hydrodynamic instabilities are usually developing and produce a phenomenon called Angle Vortex Shedding (AVS). In SRMs, such unsteady flow can be coupled with the acoustic of the chamber. The original design of the C1 aimed at exciting the first axial acoustic mode in single phase flow thanks to the AVS [17]. To do so, a sharp discontinuity is placed at the center of the combustion chamber. Unexpectedly however, various numerical simulations [18, 11] proved that the second axial mode is excited providing a distinctive monochromatic pressure oscillation at the head-end, independently of the numerical method.

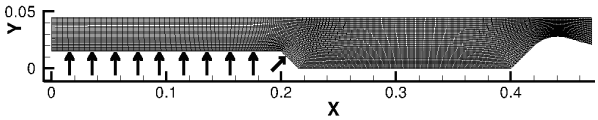

Figure 1: 317×30 mesh of the C1 with inlet indication

In a preliminary investigation, both MacCormack and MUSCL methods are used on the single phase case of [17] on the 317×30 cells mesh presented in Figure 1. In accordance with [17, 18, 11] we find a monochromatic instability around $2650H_z$. Negligible differences on this value are obtained using the MacCormack and MUSCL methods. Moreover, a mesh convergence analysis until a 2536×240 mesh leads to the conclusion that the results using the standard mesh already were of high quality and can be considered as converged.

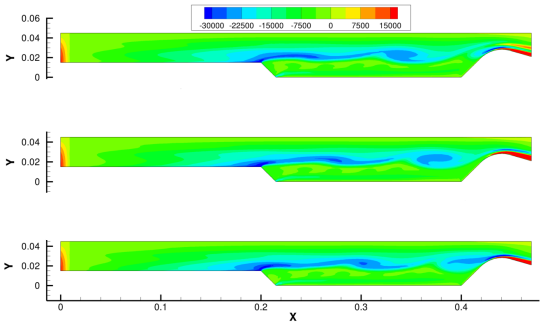

Figure 2: Gas rotational field evolution with $5\mu m$ particles and MK model at time (up to bottom) $t = 0\mu s$, $t = 147\mu s$, $t = 294\mu s$

In [18], particles are injected such that the particle to gas mass ratio $\frac{\dot{m}_p}{\dot{m}_g} = 0.396$ corresponds to a propellant using 15 % of aluminum powder. Such high presence of particles have a notable impact on the instability amplitude and frequency. As an example, the injection of $5\mu m$ particles creates a shift in frequency to approximately $2250H_z$ as well as a reduction by almost the half of the oscillation magnitude. The development of the corresponding gas rotational field is presented in Figure 2. Using the two-phase acoustic theory of [23], one can estimate that the injection of $16\mu m$ particles will attenuate the AVS with the highest efficiency. Numerical experiments using both a MUSCL type of scheme [18] and MacCormack scheme [5] on the mesh presented in Figure 1 reported that the instability completely vanish for this size. This behavior can be observed on a close range of particle diameter around to $16\mu m$. For the numerical experiment presented hereafter, $20\mu m$ particles are injected. For such size, the detection and occurrence of AVS is not ensured creating a discriminant situation.

4.2. Solutions using the monokinetic closure

In order to validate the results obtained on the standard mesh of the cited paper, we conduct a mesh refinement for the various numerical strategies. To stay consistent with the previous investigation, the equations of pressureless gas dynamics are used. A first test using a MacCormack scheme for both phases as in [5] indicates a steady engine. The flow obtained exhibits a local high mass concentration near the symmetry axis and close to the nozzle inlet.

Among the possibilities at our disposal, we chose the combinations of upwind schemes (first order and MUSCL) for the droplets and MUSCL or MacCormack schemes for the carrier

phase. It is important to note that the computation involving the MacCormack scheme for gas has been conducted with the in-house code SIERRA whereas the semi-industrial software CEDRE has been used for the fully upwind configurations. The result on the most refined mesh has been conducted with CEDRE since it allows us to finalize the simulation within a reasonable computational time. The characteristics of the AVS, when detected, are given Table 1.

The results shows that the AVS is only detected using an accurate method for the carrier phase and the disperse phase only. If the first order method is known to be highly diffusive, the MacCormack scheme is impacted by the artificial viscosity, which is needed for stability issues. Its effect is especially important close to high density gradient and vacuum due to the sensor chosen. At the same locations, the multislope MUSCL method accurately solves the flow avoiding spurious and dissipative effects. We conclude that combined with the physical dissipation due to the presence of the particles, the resulting numerical dissipation has a strong impact and can make the AVS disappear.

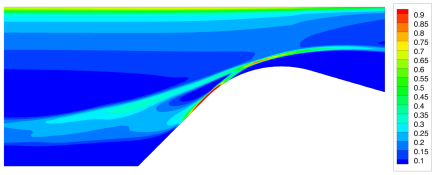

Figure 3: Dynamic PTC in the convergent

Aside the numerical strategy for the disperse phase, the impact of the carrier phase resolution can be observed when the AVS is detected. Since this MUSCL version is LED and thus dissipates at extrema, the pressure amplitude obtained are lower than for the MacCormack scheme. Thanks to the low dissipation of the setup, a tiny instability can be detect thanks to the coarsest mesh but only correctly resolved on a refined one. Besides, the frequency observed indicates that two distinct phenomena are detected. According to the previous study, frequencies close to $2150Hz$ matching the second axial mode are expected. However the $1450Hz$ instability does not correspond to any acoustic mode of the chamber. A closer look to the density field in that case indicates the occurrence of δ-shocks that are consequences of PTC, which can not be represented using a monokinetic model. These singularities take their origin in two distinct phenomena. On the one hand, the nozzle geometry leads to the crossing of the particles coming from the head-end of the engine with those deviated by the convergent in a quasi-stationary crossing phenomenon. On the other hand, the AVS causes the ejection of the particles from the vortices and thus their impact on the wall and symmetry axis as well as the dynamical crossing of their trajectories as it can be seen in Figure 3. Even if further studies are to be conducted in order to obtain firm conclusion, we can anticipate that this last phenomenon is the main cause of the shift in frequency.

4.3. Solutions using the anisotropic Gaussian closure

In order to go over the influence and limitations of such singularities, which are only due to model limitations, we propose to replace the MK equations by the AG model. Due to the additional realizability constraints compared to the equations of pressureless gas dynamics, only the MUSCL scheme can be used for the resolution of the disperse phase. Moreover since this new model is not yet implemented in CEDRE, the in-house code SIERRA is the only one which can be used and thus the MacCormack scheme solves the carrier phase in our new configuration. We expect reliable results from this combination.

A first test on the coarsest mesh does not conduct to the detection of AVS. The possibility of the new model to take into account trajectory crossing results in a spatial redistribution of particles, thus avoiding artificial particle high concentrations, but thus leading to an effect, which is close to the previous artificial dissipation. The velocity dispersion is mainly observed at the stationary crossing around the nozzle and in a more marginal way at the symmetry axis.

Thanks to the refined mesh (634×60), the simulation are conducted starting from an initial condition involving the MK closure. The action of the velocity dispersion when PTC is encountered can be seen in Figure 4. We observe an immediate transition to a new unsteady regime of approximately $2100H_z$ at a lower average pressure with $\sqrt{2}RMS = 8mbar$. Since the state of the art in this field of research clearly states that the magnitude of oscillations are hard to predict [21], we are not for now able to clearly assess the obtained improvement. However, the fields resolved provide less artifact of the model, which supposes an higher reliability of these new results, even if further detailed analysis are to be conducted in order to draw some firmer conclusions on the coupled effects of modeling and numerical strategy.

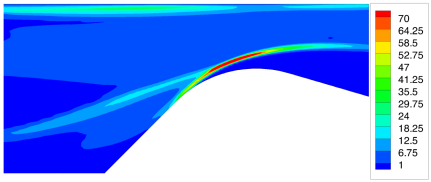

Figure 4: σ_{22} velocity dispersion in the nozzle

5. Conclusion

In this contribution, we have introduced both a new numerical strategy as well as a new Eulerian model, able to cope with PTC while preserving a well-posed mathematical system of PDEs for which an entropy inequality guarantees a proper treatment of natural singularities, which are inherent to fully Eulerian modeling of disperse two-way coupled two-phase flows. A discriminant test-case in the field of solid propulsion has been adequately chosen in order to conduct a study on the influence of both modeling and numerical methods.

We conclude this paper by observing the critical influence of both the modeling and the numerics. The interest of realizable methods has been pointed out since they are the only ensuring reliable solution when singularities occur, even locally. As far as the monokinetic model is concerned, the strong singularities resulting from the inertia of the particles and from PTC leads to strong singularities, δ-shocks, the effect of which can not completely be dealt without using adequate numerical methods. The AG level of modeling provides an interesting alternative in order to avoid such singularities but the gain in predictivity for actual SRMs simulations still requires further investigations.

While the detailed studies we are conducting are of real importance in the C1 configuration in order to draw some firm conclusions of the influence of both modeling and numerical methods for the prediction of instabilities, comparisons and validations relying on experimental measurements are necessary. We then have to switch to at least 2D axi-symmetrical configurations or even 3D axi-symmetrical configurations and this requires some further development in terms of models and realizable numerical methods, which is work in progress. It should provide a clear assessment of the improvement of the predictive character of the simulations using a tailored strategy involving the right level of modeling resolved using robust and accurate parameter-free numerical simulations.

Table 1: Instability characteristics depending on the numerical strategy using the monokinetic closure

Mesh	$\mathcal{T}_p$	$\mathcal{T}_g$	Main frequency	$\sqrt{2}RMS\ (mbar)$
(317×30)	First order	MacCormack	-	-
	MacCormack	MacCormack	-	-
	Multislope	MacCormack	$2121 \pm 16\,Hz$	0.2625
	Multislope	Multislope	-	-
(634×60)	First order	MacCormack	-	-
	MacCormack	MacCormack	-	-
	Multislope	MacCormack	$1463 \pm 13\,Hz$	17.8
	Multislope	Multislope	$2173 \pm 13\,Hz$	6.21
(1268×120)	Multislope	Multislope	$1430 \pm 35\,Hz$	5.57

References

[1] M. Boileau, L. Lagarde, V. Dupif, F. Laurent, and M. Massot. Two-size moment Eulerian multi-fluid method describing the statistical trajectory crossing: modeling and numerical scheme. In *9th ICMF, Firenze*, 2016.

[2] F. Doisneau. *Modeling and simulation of polydisperse moderately dense coalescing spray flows with nanometric-to-inertial droplets: application to Solid Rocket Motors*. PhD thesis, Ecole Centrale Paris, 2013. TEL : https://tel.archives-ouvertes.fr/tel-01009896.

[3] F. Doisneau, F. Laurent, A. Murrone, J. Dupays, and M. Massot. Eulerian Multi-Fluid models for the simulation of dynamics and coalescence of particles in solid propellant combustion. *Journal of Computational Physics*, 234:230–262, 2013.

[4] F. Doisneau, A. Sibra, J. Dupays, A. Murrone, F. Laurent, and M. Massot. Numerical strategy for unsteady two-way coupled polydisperse sprays: application to solid-rocket instabilities. *Journal of Propulsion and Power*, 30(3):727–748, 2014.

[5] J. Dupays. *Contribution à l'étude du rôle de la phase condensée dans la stabilité d'un propulseur à propergol solide pour lanceur spatial*. PhD thesis, Institut National Polytechnique de Toulouse, 1996.

[6] O. Emre, D. Kah, S. Jay, Q.-H. Tran, A. Velghe, S. De Chaisemartin, R.O. Fox, F. Laurent, and M. Massot. Eulerian moment methods for automotive sprays. *Atomization and Sprays*, 25:189–254, 2015.

[7] S. Gottlieb. On high order strong stability preserving Runge–Kutta and multi step time discretizations. *Journal of Scientific Computing*, 25(1):105–128, 2005.

[8] J.-F. Guery et al. Solid propulsion for space applications: An updated roadmap. *Acta Astronautica*, 66(1):201–219, 2010.

[9] A. Jameson. Positive schemes and shock modelling for compressible flows. *International Journal for Numerical Methods in Fluids*, 20(8-9):743–776, 1995.

[10] D. Kah, F. Laurent, M. Massot, and S. Jay. A high order moment method simulating evaporation and advection of a polydisperse liquid spray. *Journal of Computational Physics*, pages 231(2):394–422, 2012.

[11] A. Kourta. Computation of vortex shedding in solid rocket motors using time-dependant turbulence model. *Journal of Propulsion and Power*, 15(3):390–400, 1999.

[12] P. Kuentzmann. Instabilités de fonctionnement des systèmes propulsifs. *La Recherche Aérospatiale*, 5:341–351, 1995.

[13] F. Laurent and M. Massot. Multi-fluid modeling of laminar poly-dispersed spray flames: origin, assumptions and comparison of the sectional and sampling methods. *Comb. Theory and Modelling*, 5:537–572, 2001.

[14] F. Laurent, A. Sibra, and F. Doisneau. Two-size moment multi-fluid model: a robust and high-fidelity description of polydisperse moderately dense evaporating sprays. *To appear, Commun. Comput. Phys.*, pages 1–42, 2015. HAL: https://hal.archives-ouvertes.fr/hal-01169730/en.

[15] C. Le Touze, A. Murrone, and H. Guillard. Multislope MUSCL method for general unstructured meshes. *Journal of Computational Physics*, 284:389–418, 2015.

[16] C.D. Levermore and W.J. Morokoff. The Gaussian moment closure for gas dynamics. *SIAM J. Appl. Math.*, 59(1):72–96, 1998.

[17] N. Lupoglazoff and F. Vuillot. Numerical simulation of vortex-shedding phenomena in 2D test case solid rocket motors. In *30th Aerospace and Sciences Meeting and Exhibit*, 1992.

[18] V. Morfouace and P.-Y. Tissier. Two-phase flow analysis of instabilities driven by vortex-shedding in solid rocket motors. In *31st AIAA/ASME/SAE/ASEE Joint Propulsion Conference and Exhibit*, 1995.

[19] M. Sabat. *Eulerian models and realizable numerical schemes for the description of low-to-medium inertia polydisperse sprays in turbulent two-phase flows*. PhD thesis, Université Paris-Saclay, 2016.

[20] M. Sabat, A. Vié, A. Larat, and M. Massot. Fully Eulerian simulation of 3D turbulent particle laden flow based on the Anisotropic Gaussian Closure. In *9th ICMF, Firenze*, 2016.

[21] A. Sibra. *Modélisation et étude de l'évaporation et de la combustion de gouttes dans les moteurs à propergol solide par une approche eulérienne Multi-Fluide*. PhD thesis, Université Paris-Saclay, 2015. available on TEL https://tel.archives-ouvertes.fr/tel-01260314.

[22] R.C. Swanson and E. Turkel. On central-difference and upwind schemes. *Journal of computational physics 101,292-306*, 1991.

[23] S. Temkin and R. A. Dobbins. Attenuation and dispersion of sound by particulate-relaxation processes. *The Journal of the Acoustical Society of America*, 40(2):317–324, 1966.

[24] E. F. Toro. *Riemann Solvers and Numerical Methods for Fluid Dynamics: A Practical Introduction*. Berlin, Heidelberg: Springer-Verlag Berlin Heidelberg, 2009.

[25] A. Vié, F. Doisneau, and M. Massot. On the Anisotropic Gaussian closure for the prediction of inertial-particle laden flows. *Commun. Comput. Phys.*, 17(1):1–46, 2015.